Journal of Sea Research xxx (2014) xxx–xxx

Contents lists available at ScienceDirect

Journal of Sea Research

journal homepage: www.elsevier.com/locate/seares

Simple measurements reveal the feeding history, the onset of reproduction, and energy conversion efficiencies in captive bluefin tuna

Marko Jusup [a,*], Tin Klanjšček [b], Hiroyuki Matsuda [c]

[a] Department of Biology, Kyushu University, 6-10-1 Hakozaki, Higashi Ward, Fukuoka 812-8581, Japan
[b] Department for Marine and Environmental Research, Rudjer Boskovic Institute, Bijenicka 54, 10000 Zagreb, Croatia
[c] Graduate School of Environment and Information Sciences, Yokohama National University, 79-7 Tokiwadai, Hodogaya Ward, Yokohama 240-8501, Japan

ARTICLE INFO

Article history:
Received 24 March 2014
Received in revised form 3 September 2014
Accepted 10 September 2014
Available online xxxx

Keywords:
Dynamic Energy Budget
Model validation
Aquaculture
Thunnus orientalis
Feeding
Maturation

ABSTRACT

We present a numerical approach that, in conjunction with a fully set up Dynamic Energy Budget (DEB) model, aims at consistently approximating the feeding history of cultivated fish from the commonly measured aquaculture data (body length, body mass, or the condition factor). We demonstrate the usefulness of the approach by performing validation of a DEB-based model for Pacific bluefin tuna (*Thunnus orientalis*) on an independent dataset and exploring the implied bioenergetics of this species in captivity. In the context of validation, the results indicate that the model successfully accounts for more than 75% of the variance in actual fish feed. At the 5% significance level, predictions do not underestimate nor overestimate observations and there is no bias. The overall model accuracy of 87.6% is satisfactory. In the context of tuna bioenergetics, we offer an explanation as to why the first reproduction in the examined case occurred only after the fish reached seven years of age, whereas it takes five years in the wild and sometimes as little as three years in captivity. Finally, we calculate energy conversion efficiencies and the supply stress throughout the entire lifetime to theoretically underpin the relatively low contribution of growth to aerobic metabolism implied by respirometry and high feed conversion ratio observed in bluefin tuna aquaculture.

1. Introduction

Global decline of wild bluefin tuna populations (Collette et al., 2011; Juan-Jordá et al., 2011) makes aquaculture an increasingly attractive alternative to fisheries. However, bluefin tuna aquaculture faces numerous challenges. For example, tunas are top predators, requiring large amounts of highly caloric feed that increase operational costs sometimes to the point of making aquaculture economically non-competitive. Furthermore, tunas are notoriously difficult to breed in captivity, causing aquaculture to depend on the collapsing wild stocks for juveniles and thus threatening sustainability of production.

Much – mostly experimental – research has been conducted to overcome these problems. The research has largely been devoted to improving the sustainability of production (Iioka et al., 2000; Miyake et al., 2003; Mylonas et al., 2010), devising formulated feeds (Carter et al., 1999; Ji et al., 2008; Mourente and Tocher, 2009), and closing the life-cycle in captivity (De Metrio et al., 2010; Grubišić et al., 2013; Masuma et al., 2008, 2011; Sawada et al., 2005). However, experimental studies on tuna are expensive and only relevant for the set of environmental conditions used in the study, thus making tests of alternative scenarios difficult.

Theoretical approaches based on Dynamic Energy Budget (DEB) theory (Kooijman, 2010; Nisbet et al., 2000; Sousa et al., 2008, 2010) have proven effective in transcending these issues. DEB-based models help advance our understanding of organismal processes such as energy acquisition, utilization, and the resulting growth by re-interpreting the data using rules common to all life. The models have already been used to successfully investigate numerous fish-related problems (Augustine et al., 2011, 2012; Freitas et al., 2012; Serpa et al., 2012; Teal et al., 2012; Einarsson et al., 2011; Fablet et al., 2011; Pecquerie et al., 2009, 2011; van der Meer et al., 2011; van der Veer et al., 2009).

Here we develop and, with the help of data commonly measured at aquaculture facilities, make use of a DEB-based theoretical approach to improve our understanding of bluefin tuna growth in aquaculture. We start from an existing full life-cycle bioenergetic model for bluefin tuna (Jusup et al., 2011), interpret the model in an aquaculture setting to enable reconstruction of the feeding history during the cultivation cycle, validate the model, and use the validated model to investigate energy conversion efficiency of Pacific bluefin tuna (*Thunnus orientalis*, hereafter PBT) in captivity. Available data, the DEB-based model for PBT, statistical methods for model validation, methods for the feeding history reconstruction, and methods for calculating energy conversion efficiency are described in the Methods section. The Results and discussion section contains an overview of the results and a detailed discussion providing the context. In particular, we emphasize how simple

* Corresponding author. Tel.: +81 926422641.
E-mail address: mjusup@gmail.com (M. Jusup).

http://dx.doi.org/10.1016/j.seares.2014.09.002
1385-1101/

measurements reveal the feeding history and the onset of reproduction in captive PBT, and discuss the limits of the approach. The Conclusion section summarizes the findings and suggests priorities for future research.

2. Methods

2.1. Data on captive Pacific bluefin tuna

Applying an existing DEB-based model for PBT to an aquaculture setting involved using two types of data. First, simple measurements on captive PBT (e.g. body length, body mass, or the condition factor) were needed to reconstruct the feeding history. Second, actual feeding records were needed to compare the reconstructed feeding history against the data, and ultimately validate the model. Such data – pertaining to a broodstock maintained for 13 years by Kinki University near Kushimoto, Wakayama Prefecture, Japan – were reported by Miyashita (2002). In particular, out of 3221 young juveniles caught in Aug–Sept 1987 and placed in 12 m wide and 6 m deep square net pens, 2354 individuals surviving the first week in captivity were used for rearing. After two months, the surviving fish were relocated and thereafter permanently kept in larger 31 m wide and 11 m deep square net pens. Readily available annual data (Miyashita, 2002) included survival, mass of distributed fish feed, and average body mass (Table 1). The average condition factor had to be estimated from a graph. We used average body mass and the condition factor to back-calculate body length representative of the fish in net pens.

Diet composition in terms of the percentage of distributed fish feed was also available (Table 2). An eight-year long time series showed that the daily average sea-water temperature at the rearing facility oscillated sinusoidally between 16 and 26 °C over the year. There were no large differences in the daily averages at the surface and 5 m deep. Lastly, the first spawning event was observed in July 1994 when the fish was approximately seven years and two months old. For further details (and wealth of information on handling artificially spawned larval PBT) the reader may want to consult the publication by Miyashita (2002).

2.2. Model description

We use a complete life cycle DEB-based model for PBT developed by Jusup et al. (2011) shown in Fig. 1. The model has three state variables: (i) energy reserves, E, representing the amount of energy potentially available to metabolic processes; (ii) the structural volumetric length, L, measuring the amount of energy embedded into the structure, and (iii) the level of maturity, E_H, tracking the developmental state of fish.

Table 1
Data on growth of captive PBT as reported by Miyashita (2002): the case of a broodstock maintained for 13 years by Kinki University near Kushimoto, Wakayama Prefecture, Japan.

Age	Number of individuals[a]	Mass of feed (kg)	Average body mass (kg)	Average condition factor[b]	Average fork length (cm)[c]
0	2354	50,989	0.26	1.57	25.5
1	1224	117,176	8	1.99	73.8
2	905	126,058	12	2.00	84.4
3	765	122,570	20	2.02	99.7
4	631	149,101	30	2.04	114
5	598	154,241	40	2.07	125
6	321	155,792	57	2.10	140
7	281	163,303	75	2.13	152
8	171	96,307	90	2.18	160
9	99	66,814	120	2.23	175
10	93	82,597	150	2.28	187
11	76	74,116	180	2.34	198
12	63	41,506	220	2.40	209

[a] At the beginning of the period.
[b] Estimated (except age 0).
[c] Back-calculated from average body mass and the average condition factor (except age 0).

Table 2
Data on feeding of captive PBT as reported by Miyashita (2002): the case of a broodstock maintained for 13 years by Kinki University near Kushimoto, Wakayama Prefecture, Japan.

Age	Sardine[a]	Sand lance	Horse mackerel	Mackerel	Cuttlefish	Bonito & other bait fish
0	57.5	42.4	0.1	–	–	–
1	85.9	–	12.8	0.5	<0.1	0.8
2	66.5	–	1.3	7.7	<0.1	24.5
3	5.2	0.5	17.4	11.6	0.2	65.1
4	43.5	–	15.6	35.9	<0.1	5.1
5	43.8	–	11.1	32.3	4.3	8.5
6	6.9	–	27.7	53.6	4.1	7.7
7	2.5	–	11.0	77.0	9.3	0.2
8	4.6	–	27.4	63.2	4.7	–
9	2.0	–	14.9	77.0	6.0	0.1
10	0.5	–	9.7	84.6	5.3	–
11	0.2	–	6.8	88.8	4.2	–
12	3.5	–	0.3	84.1	9.1	3.0

[a] Entires in this and all subsequent columns are given as a percentage of feed mass from Table 1.

The dynamics of the three state variables are determined by six energy flows (please see Appendix A for details):

- Assimilation flow, $\dot{p}_A$: the rate of energy entering the reserve due to feeding.
- Utilization (mobilization or catabolic) flow, $\dot{p}_C$: the rate of utilization (or mobilization) of energy from the reserve. The utilization flow is assumed to be split according to the κ-rule: the fraction $\kappa\dot{p}_C$ serves the needs for somatic maintenance and fuels growth if there is energy available. The remaining fraction, $(1-\kappa)\dot{p}_C$, satisfies the needs for maturity maintenance and, depending on the current level of maturity, fuels maturation or reproduction if there is energy available.
- Somatic maintenance flow, $\dot{p}_S$: the flow of energy required to sustain a fish.
- Maturity maintenance flow, $\dot{p}_J$: the flow of energy required to maintain the level of maturity.
- growth flow, $\dot{p}_G$, the flow of energy into the structure when $\kappa\dot{p}_C > \dot{p}_S$, leading to the increase in the structural length (L).
- Maturation/reproduction flow, $\dot{p}_R$: if $(1-\kappa)\dot{p}_C > \dot{p}_J$, energy left over from maturity maintenance, $(1-\kappa)\dot{p}_C - \dot{p}_J$, is committed to maturation until $E_H < E_H^p$, and to reproduction afterwards.

2.3. Supplementary assumptions

Though our model was inspired by the standard DEB representation (Kooijman, 2010) and its application to small pelagic fish (Pecquerie et al., 2009), the characteristic physiology of PBT required three

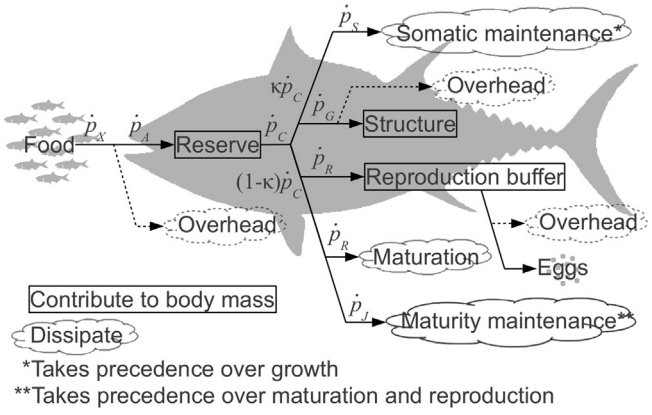

Fig. 1. A schematic representation of the DEB-based model for bluefin tuna. Assimilation, growth, and reproduction overheads are paid directly from the corresponding energy flows. Somatic and maturity maintenance flows, the maturation flow, and overheads represent the dissipated energy, and therefore contribute to the respiration rate.

Please cite this article as: Jusup, M., et al., Simple measurements reveal the feeding history, the onset of reproduction, and energy conversion efficiencies in captive bluefin tuna, J. Sea Res. (2014), http://dx.doi.org/10.1016/j.seares.2014.09.002

supplementary assumptions on morphology and thermogenesis. These assumptions and the underlying physiological evidence were discussed by Jusup et al. (2011) in detail; we only list them briefly here.

First, we assumed that soon after hatching larval PBT increase assimilation and utilization proportionally with L^3, rather than L^2 as in the standard DEB model. For around 30 days after hatching, larval PBT exhibit the near-exponential growth (Miyashita, 2002; Miyashita et al., 2001; Sawada et al., 2005). DEB theory offers several scenarios that account for the near-exponential growth in fish (Kooijman et al., 2011), but physiological evidence suggests that increasingly efficient energy assimilation and utilization are responsible, i.e. a type M acceleration of growth observed in many fish species (Lika et al., in press). During the exponential growth, multiple physiological changes thought to improve food assimilation and ingestion have been observed. For example, the first appearance of gastric glands and pyloric caeca, together with a sharp increase in the specific activity of trypsin-like and pepsin-like digestive enzymes, points to an improvement in food assimilation (Kaji, 2003). Simultaneously, the larvae undertake a number of anatomical transformations that represent an improvement in food ingestion ability (Miyashita, 2002): allometric (i.e. non-isomorphic) growth of the preanal length, head length and height, snout and upper jaw length, and the eye diameter. Observations suggest increase in energy utilization from the reserve as well. Larval PBT, in comparison with other previously examined fish species, exhibit a very high (and increasing) ratio of the growth hormone immunoreactive cell volume to the pituitary volume, %GH (Kaji, 2003).

Second, we adjusted parameters to account for the changes in the shape. Standard DEB assumes isomorphic growth, i.e. growth in which the ratio of any two different lengths (e.g. the ratio of preanal to head length) is constant. The abovementioned anatomical transformations clearly show that tuna is not growing isomorphically in the early stages of growth. Consequently, the structural volumetric length could not be held strictly proportional to any measurable physical length, as would be the case with an isomorph in the standard DEB representation. Jusup et al. (2011) found that the PBT growth data could be fitted nicely using a non-linear relationship between structural volumetric and fork lengths consistent with the observed rapidly changing shape during the early development and an asymptotic approach to the final shape later.

Third, the standard DEB representation needed an adjustment to properly account for the role of excess red muscle tissue in continuous swimming and, consequently, thermogenesis (Graham and Dickson, 2004; Katz, 2002). Three interconnected mechanisms were identified as critical in the context of thermogenesis: (i) the requirement that all tunas swim continuously (Magnuson, 1973; Roberts, 1975), (ii) steady source of heat due to inefficiency of (excess) red muscle tissue in chemical-to-kinetic energy conversion (Graham and Dickson, 2001, 2004; Smith et al., 2005), and (iii) heat conservation by countercurrent vascular heat exchangers, rete mirabile (Graham and Dickson, 2001, 2004). For the model construction it was crucial to account for metabolic costs, thus prioritizing mechanism (ii), particularly the observations that showed marked changes in metabolism of juvenile tuna coinciding with the onset of thermogenesis and red muscle development. For instance, a steep drop in the daily growth rates of juvenile PBT was found to occur within 90 to 120 days after hatching (Miyashita, 2002). Furthermore, Kubo et al. (2008) observed that thermogenesis in PBT became measurable at slightly less than 20 cm fork length (<80 days after hatching) and was readily detectable in fish of over 40 cm fork length (>120 days after hatching). At the same time, the volume ratio of red to white muscle was observed to increase non-linearly with the body length reaching a maximum of around 12% at close to 50 cm fork length. Nisbet et al. (2012) augmented this evidence with a review of related issues and concluded that a large fraction of energy assimilated by PBT was lost in the form of heat (and metabolic products) originating from continuous swimming powered by the red muscle tissue. Hence, we assumed that, at the onset of thermogenesis, the somatic maintenance costs of PBT increased considerably in accordance with a term proportional to the squared structural length.

2.4. Relating data to state variables

The state variables of any DEB-based model, including the present model for PBT, are abstract quantities in the sense that they cannot be directly measured. For practical use, therefore, we need to convert the state variables to some readily measurable quantities. Typically, the latter can be expressed as explicit functions of the former. Because we are applying the model in conjunction with data from aquaculture (Table 1), the conversion of the state variables into fork length, body mass, and the condition factor is of primary interest.

Structural length (L) of an organism in DEB is related to the organism's physical length (L_w) through the shape factor, δ_M. In isomorphic organisms the two lengths are proportional and δ_M is just a constant. Because tuna changes its shape as it matures, the shape factor is a function of maturity (see Appendix A for details), $\delta_M \equiv \delta_M(E_H)$, and the fork length is given by:

$$L_w = \frac{L}{\delta_M(E_H)}. \tag{1}$$

Body mass of the organism is calculated by summing up contributions from all relevant DEB state variables: reserve, structure, and (in adults) the reproductive buffer:

$$W = d_V L^3 + \rho_E(E + E_R), \tag{2}$$

where d_V is the density of the structure and ρ_E is the mass-energy coupler for the reserve.

The condition factor, K, is extensively used to characterize the condition of the fish, $K = CW/L_w^3$, where C is a scaling constant used to bring the value of K close to unity (Nash et al., 2006). In the context of DEB theory, the condition factor quantifies the abundance of the reserve relative to the structure (Bavčević et al., 2010). The relationship can be seen after combining Eqs. (1) and (2):

$$K = C(\delta_M(E_H))^3\left(d_V + \rho_E\frac{E + E_R}{L^3}\right), \tag{3}$$

which shows that K is a function of the ratio of total energy reserves ($E + E_R$) and the structural volume. In bluefin tuna aquaculture, C is typically set to $C = 10^5\ \mathrm{cm^3 \cdot kg^{-1}}$.

Eqs. (1)–(3) represent a recipe for the conversion of the abstract state variables into quantities that are commonly measured in fish aquaculture. With such a recipe in hand, we can proceed to describe the algorithm for the reconstruction of the feeding history in captive PBT.

2.5. Reconstruction of the feeding history

We reconstruct the feeding history of captive PBT from the data in Table 1 using a step-by-step estimation algorithm. Our aim is to generalize a feeding history reconstruction method presented in Kooijman (2010). The Kooijman's method makes use of a single source of information (i.e. a time series of measurements) in conjunction with a DEB model to calculate unique food availability, $0 \le f \le 1$, as a function of time, $f = f(t)$. The reconstructed $f(t)$ always gives a perfect fit of the original time series; for example, a time series of body mass measurements as a source of information is perfectly fitted with the body mass calculated by plugging the reconstructed $f(t)$ back into the DEB model. Rather than limiting ourselves to just one, we include multiple sources of information (indexed $i = 1, \ldots, N$) into the feeding history reconstruction. The reason for doing so is that, if the model represents the real fish well, the model's results are expected to be in good agreement with

Please cite this article as: Jusup, M., et al., Simple measurements reveal the feeding history, the onset of reproduction, and energy conversion efficiencies in captive bluefin tuna, J. Sea Res. (2014), http://dx.doi.org/10.1016/j.seares.2014.09.002

several time series simultaneously, rather than in perfect agreement with just one. Consequently, our method does not come with a unique solution in itself, but depends on the selection of an objective function that is used during the reconstruction. The objective function quantifies the model error (i.e. the "distance" between model outputs and measurements) for which a definitive mathematical expression does not exist. Hence, we select one possible alternative that is relatively straightforward to implement. Starting the reconstruction in a manner similar to Kooijman (2010), we fit a spline that preserves monotonicity and the shape of the data (for definitions see Fritsch and Carlson, 1980) to each time series of measurements to create a set of interpolants $d_i(t)$, $i = 1, \ldots, N$. We then numerically integrate the DEB model for PBT, where at each integration step an output, $e_i(t)$, $i = 1, \ldots, N$, comparable to $d_i(t)$, $i = 1, \ldots, N$ is generated (e.g. if $d_i(t)$ comes from a time series of body mass measurements, then $e_i(t)$ is modeled body mass). The outputs $e_i(t)$ are obtained by converting the model state variables into measurable quantities using Eqs. (1)–(3). Because $e_i(t)$ depend on food availability, an objective way of choosing $f(t)$ is needed for the numerical integrator to advance from one step to another. Assuming that the state variables at time $t - 1$ are known, the integration step to the next moment t is performed with food availability that minimizes the objective function $\max_i F_i(f|t)$, where $F_i(f|t) = C_i|d_i(t) - e_i(t)|$. Weights, C_i, $i = 1, \ldots, N$, equalize differences in scale across the available time series of measurements. Generally, weights can be functions of time, i.e. $C_i = C_i(t)$. The described minimization problem is solvable using sequential quadratic programming method (Boggs and Tolle, 1995). By solving the same problem for all t, we obtain a step-by-step estimate of the feeding history from readily available measurements, in our case average body mass and the average condition factor (Table 1). Using the introduced notation, $d_1(t) = W(t)$ and $d_2(t) = K(t)$, where W and K stand for body mass and the condition factor from Table 1, respectively. The corresponding weights are $C_1 = C_W = 1$ and $C_2 = C_K = 100$. The reconstruction is initialized by running the model at constant food availability, $f_0 = 0.820$, and temperature, $T_0 = 27.5$ °C (Chen et al., 2006), from $t_0 = 0$, marking the beginning of embryo development inside the egg, to $t_1 \approx 90$ days, marking the first available data point. Without any reference on food availabilities experienced by PBT in larval and early juvenile stages in the ocean, the value of f_0 is chosen simply to guarantee continuity in the sense of $f_0 \approx f(t_1)$, where $f(t_1)$ is the result of the first reconstruction step.

Following the reconstruction of the feeding history in terms of food availability (f), we convert the results into the estimates of the actual feed mass ingested by the fish, W_X. Such estimates can then be compared to the actual reported values (Table 1) to evaluate the model performance. We convert f into W_X using the following formula:

$$W_X = \frac{\rho_X}{\kappa_X} \int \dot{p}_A(f) N(t) dt, \tag{4}$$

where $N(t)$ is the number of individuals held captive at time t, κ_X ($0 < \kappa_X \leq 1$, see Appendix A for details) is the constant assimilation efficiency of food into the reserve, and ρ_X is the mass-energy coupler for food. Note that the ratio $\dot{p}_A/\kappa_X$ used in Eq. (4) is the ingestion rate of an individual fish that, when multiplied with the current number of fish ($N(t)$), gives the total amount of ingested energy per unit of time. To obtain the grand total energy ingested by the tuna, we integrate over a time period of interest. Finally, multiplication by ρ_X converts energy into mass. In Eq. (4), the role of f is to express the percentage of the maximum assimilation rate achievable at a given body length and with the quantity of food being distributed to the fish. The parameter κ_X represents a variety of metabolic constrains that cause losses of food energy from ingestion until assimilation into the reserve. The parameter ρ_X reflects food quality in terms of the energetic content. The last two parameters are explored in more details next.

We can use the estimated feed mass to evaluate the model performance and validate the model only if the two parameters in Eq. (4), κ_X and ρ_X, are estimated independently. The food conversion efficiency is supposed to account for losses associated with the inefficiencies of the digestive system and other assimilation overheads such as specific dynamic action — the transient response of respiration rate following a meal (Nisbet et al., 2012). Measurements of the apparent digestibility coefficient in Atlantic bluefin tuna, *Thunnus thynnus*, indicate that the digestibility of nitrogen, which is a proxy for protein digestibility, is in excess of 90% (Aguado et al., 2004). Hence losses in the form of feces appear to be rather low. On the other hand, measurements of specific dynamic action in southern bluefin tuna, *Thunnus maccoyii*, estimate the corresponding energy loss to be, on average, 35% (Fitzgibbon et al., 2007). Such a high estimate is somewhat at odds with the data based on the standard interpretation of respirometry for smaller yellowfin tuna, *Thunnus albacares* (Dewar and Graham, 1994; Korsmeyer and Dewar, 2001; Korsmeyer et al., 1996). These data indicate that around 18% of ingested energy is lost on specific dynamic action. Another recent study on juvenile PBT (Clark et al., 2010) reports that specific dynamic action accounts for, on average, only 9.2% of ingested energy. In view of the described uncertainties, we rather arbitrarily opt for an intermediate value and set the combined loss of ingested energy attributable to the inefficiencies of the digestive system and specific dynamic action at $\kappa_X = 0.8$. Note that κ_X is an efficiency measure, so that $1 - \kappa_X$ quantifies losses. The mass–energy coupler for food, ρ_X, is obtained by back-calculating the energy equivalent of the average chemical composition of feed used in Atlantic bluefin tuna aquaculture (Aguado-Giménez and García-García, 2003), $\rho_X = 1.894 \cdot 10^{-4}\,\mathrm{g \cdot J^{-1}}$. In units more commonly used in calorimetry measurements the last value is equivalent to $5280\,\mathrm{J \cdot g^{-1}}$, corresponding to a relatively high-energy diet.

2.6. Model validation criteria

We validate the DEB-based model for PBT using a goodness-of-fit technique (Jusup et al., 2009; Portilla and Tett, 2007). The technique consists of two steps: (i) creating an observed-vs-predicted scatter plot, and (ii) performing linear regression using the ordinary least squares (OLS) method to examine correlation between the two variables. OLS fitting provides regression coefficients, the coefficient of determination, and estimation errors.

- The regression coefficients, k and l, indicate how well the model performs over the whole prediction domain. For example, a slope coefficient (k) lower than one would reflect a situation in which the model either underestimated the observations at the low end of the domain, overestimated the observations at the high end of the domain, or both. The line intercept (l) different from zero would imply a bias in the model predictions.
- The coefficient of determination, R^2, provides an estimate of the fraction of the variance in the observations explained by the model predictions, thus giving insight into the ability of the model to capture the importance of feeding in aquaculture.
- The estimation errors help assess the model uncertainty in future applications.

We used F-statistics to conclude if the coefficient of determination was significantly different from zero. With the help of t-statistics, we calculated confidence intervals for the regression coefficients and determined whether the slope coefficient and the intercept were statistically distinguishable from one and zero, respectively. Relying on t-statistics, we calculated prediction confidence interval of the fish feed as well.

Based on the obtained results we could classify the predictive power of the model into one of the four categories (Portilla and Tett, 2007): "*good*" if R^2 is significantly different from zero and the regression line does not differ significantly from the line with slope one and intercept zero, i.e. the line of complete correspondence; "*fair*" if R^2 is significantly different from zero, but either the slope or the intercept of the regression line significantly differ from one or zero, respectively; "*poor*" if R^2 is significantly different from zero, but both the slope and the intercept

Please cite this article as: Jusup, M., et al., Simple measurements reveal the feeding history, the onset of reproduction, and energy conversion efficiencies in captive bluefin tuna, J. Sea Res. (2014), http://dx.doi.org/10.1016/j.seares.2014.09.002

of the regression line significantly differ from one and zero, respectively; and "*non-existent*" if R^2 is not significantly different from zero.

Aside from the statistical performance measures introduced above, we wanted to summarize the results of the model validation using an aggregate error (or accuracy) indicator. We found a suitable indicator in the form of the mean absolute relative error

$$E_{MAR} = \frac{1}{n}\sum_{i=1}^{n}\left|1-\frac{x_i}{y_i}\right|, \tag{5}$$

where (x_i, y_i) is the ith out of n points on the observed-vs-predicted scatter plot. From Eq. (5) we define the overall model accuracy as $A = 100\%\cdot(1 - E_{MAR})$. Note that only a perfect fit between the predictions and the observations would result in $A = 100\%$.

2.7. Energy conversion efficiencies and the supply stress

The reconstruction of the feeding history and model validation – provided both are successful – allow us to examine energy conversion efficiencies in captive PBT from a unique perspective. Here, emphasis is put on the increase of the structure (i.e. growth in length) because the mass gain potential of a fish over a given period cannot be fully realized unless growth in length is optimal (Bavčević et al., 2010). We define two conversion efficiencies in this context: instantaneous and cumulative. The instantaneous conversion efficiency, CE_1, is the ratio of growth and utilization energy flows, i.e.

$$CE_1 = \frac{\dot{p}_G}{\dot{p}_C}. \tag{6a}$$

The conversion efficiency CE_1 represents the fraction of energy mobilized from the reserve that is used for structural growth at any given moment. The cumulative conversion efficiency, CE_2, is the ratio of the total energy invested in the growth of the structure and the total energy mobilized from the reserve up to the moment t:

$$CE_2 = \frac{\int_0^t \dot{p}_G dt}{\int_0^t \dot{p}_C dt}. \tag{6b}$$

We introduce CE_2 as an integrative measure of quality of the cultivation process through time. Both conversion efficiencies are expected to decrease with food availability (f) and fish length. However, CE_1 should be much more sensitive to f than CE_2.

A quantity complementary to conversion efficiencies, comparing energy needed to run metabolic processes with energy available through assimilation, is the supply stress

$$s_s = \frac{\dot{p}_J \dot{p}_S^2}{\dot{p}_A^3}, \tag{7}$$

recently introduced in the context of a comprehensive bioenergetic comparison of five fish classes (Kooijman and Lika, in press; Lika et al., 2014). The utility of the quantity s_s stems from the fact that, at any given moment in life, the fish becomes energetically stressed (i.e. experiences starvation) when food availability and the structural length are such that $\dot{p}_S = \kappa\dot{p}_A$, at which point $\dot{p}_J \le (1-\kappa)\dot{p}_A$. Inserting these relationships into Eq. (7) we obtain $s_s \le (1-\kappa)\kappa$. Consequently, the supply stress is theoretically limited to the range from 0 to 4/27 regardless of the body length of the organism. At its high-end values, the supply stress indicates a demand-type organism, typically very active, with developed sensory organs, high peak metabolic rate, and poor handling of starvation, all of which characterize bluefin tuna quite well. Hence, it would be of some interest to quantify the supply stress for PBT and confirm whether this fish truly belongs to the demand side of the spectrum.

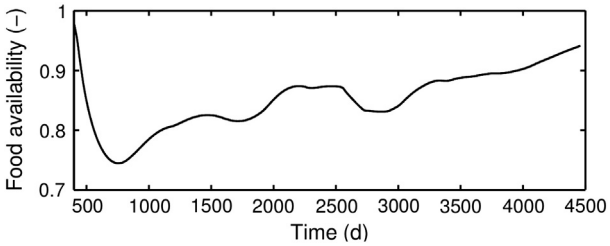

Fig. 2. Reconstructed theoretical feeding history of captive PBT expressed in terms of food availability ($0 \le f \le 1$).

3. Results and discussion

We validated a DEB-based model for PBT and used it to investigate energy conversion efficiencies in aquaculture. Model validation proceeded in two steps: (i) the reconstruction of the feeding history and (ii) the comparison of predicted with observed feeding rates, followed by a broad discussion of implications for the reared fish and an exhaustive list of limitations. Similarly, we discussed the analysis of energy conversion efficiencies in the context of aquaculture production.

3.1. Model validation

To follow the procedure described in the Methods section, we needed a DEB-based model with the set of parameters that could correctly capture PBT growth and reproduction. We used both the model and the parameters given in Jusup et al. (2011), leaving the feeding history, $f(t)$, as the sole free forcing variable. We reconstructed the theoretical feeding history, denoted $f_P(t)$ and shown in Fig. 2, by solving the minimization problem outlined above from the data on body mass and the condition factor (Table 1). Simulations based on $f_P(t)$ agreed with the observed body mass, condition factor, and fork length remarkably well (Fig. 3). The remarkable agreement, however, merely *suggested* that the model was performing as desired. A proper validation still required the confirmation of model performance on an independent dataset, i.e. mass of feed distributed to the fish during the rearing cycle (Table 1).

The observed-vs-predicted scatter plot illustrating the model performance is shown in Fig. 4 together with the corresponding regression line and the 95% prediction confidence interval. Statistical analysis (Table 3) demonstrated that the slope was not significantly different from one, and the intercept was not significantly different from zero. Therefore, the regression line was not statistically different from the line of complete correspondence. The estimate of the coefficient of determination, which was significantly different from zero, further indicated that the model captured approximately 76% of the variance in the actual fish feed. Hence, the predictive power of the model could be rated as "good", the highest category outlined by Portilla and Tett (2007). From Eq. (5), the mean absolute relative error was $\pm 12.4\%$, implying an overall model accuracy of 87.6%. The good predictive power and the satisfactory accuracy provided the necessary independent confirmation of model performance and, for the most part, concluded the validation.

Because DEB theory, in addition to growth, specifies reproduction and age-at puberty, we could look for further support for the model by comparing the predicted and observed age-at-puberty. For the given set of parameters and the reconstructed theoretical feeding history, the model predicted that the studied PBT broodstock would reach puberty 2555 days (7 years) after hatching, at around 153 cm fork length (Table 4). This prediction was surprising given the observed ages of puberty as low as 3 years, but compared very favorably with the first observed spawning of the captive broodstock, which took place on

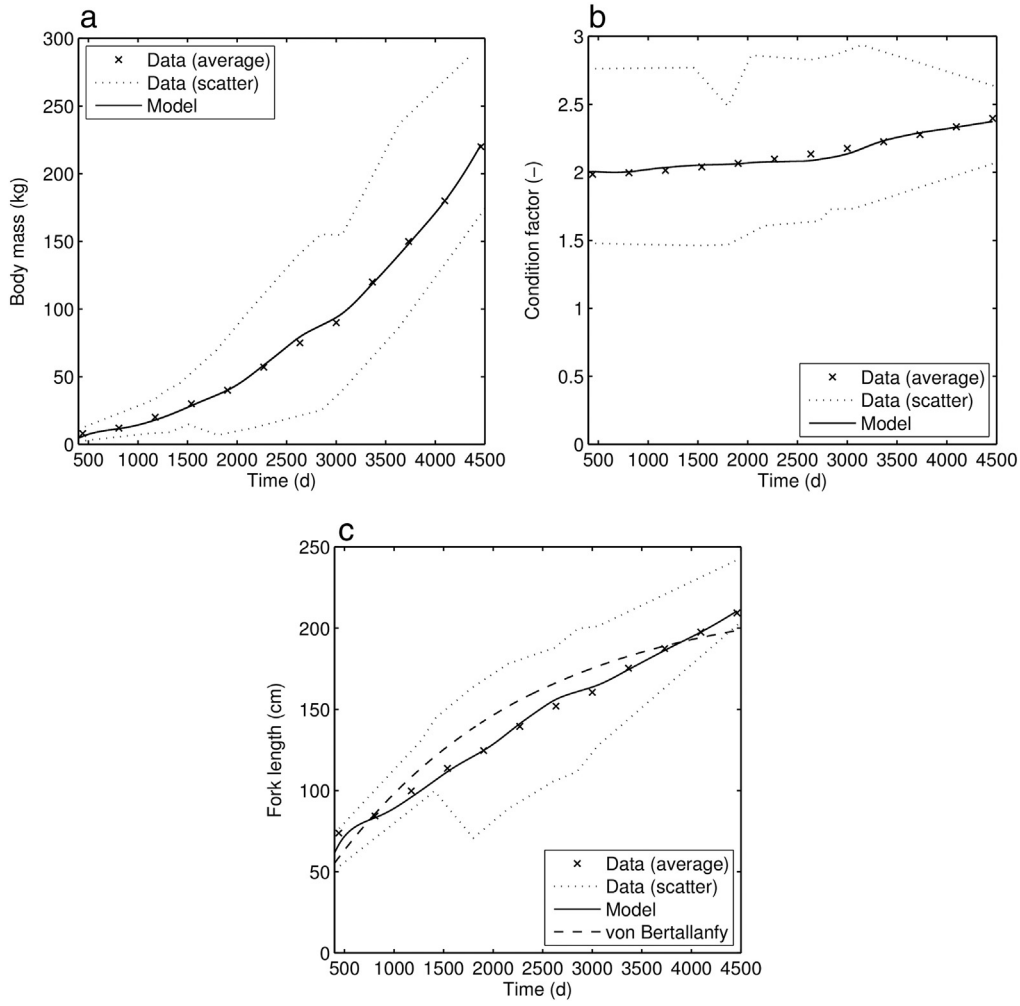

Fig. 3. Comparison of growth paths obtained from the reconstructed theoretical feeding history of captive PBT with the observations: a) body mass, b) the condition factor, and c) fork length as a function of time. The reconstruction is performed using only the data in panels a) and b). Panel c) also contains a von Bertalanffy growth curve at $f = 0.863$, i.e. the average of f displayed in Fig. 2, for reference.

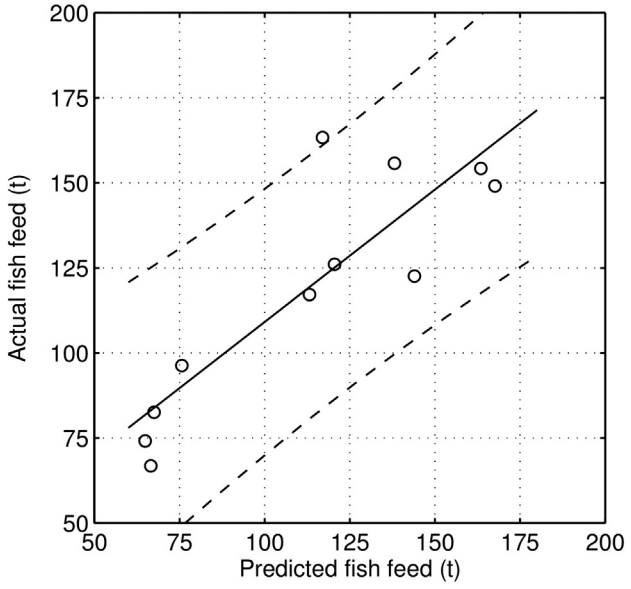

Fig. 4. Observed-vs-predicted scatter plot with the regression line obtained by the ordinary least squares method. Dashed curves represent the 95% prediction confidence interval.

July 3, 1994 when the fish was approximately seven years and two months old (Miyashita, 2002). As the information on reproduction was not used in fitting, this correspondence additionally validated the model.

DEB models predict that length of organisms follows the von Bertalanffy growth curve when food availability is constant. While tuna had been shown to follow the von Bertalanffy growth curve in many cases (Rooker et al., 2007; Shimose et al., 2009), here the body length as a function of time differed from this curve (Fig. 3c). Accordingly, we concluded that food availability was far from constant during the rearing cycle. Our feeding history reconstruction revealed the extent to which food availability oscillated through time (Fig. 2). High initial estimates ($f > 0.95$) were primarily a consequence of the data point at age 1, when the fish reportedly had an average mass of 8 kg. Such a large mass indicated that the fish responded well to a diet based on the mixture of sardine and sand lance (Table 2). By the end of the second year,

Table 3
Summary of the ordinary least squares results and accompanying statistical tests.

Coefficient	OLS estimate	Standard error	Null hypothesis	Test statistic	p-Value
Slope (k)	0.78	0.15	$k = 1$	$t = -1.51$	0.17
Intercept (l)	31.3	17.4	$l = 0$	$t = 1.79$	0.11
Determination	0.76	–	$R^2 = 0$	$F = 27.9$	<0.001

Please cite this article as: Jusup, M., et al., Simple measurements reveal the feeding history, the onset of reproduction, and energy conversion efficiencies in captive bluefin tuna, J. Sea Res. (2014), http://dx.doi.org/10.1016/j.seares.2014.09.002

Table 4
Age and length at puberty as the functions of food availability at 21 °C.

Food availability	0.80	0.85	0.90	0.95	1.00
Age-at-puberty (days)	4705	2450	1726	1341	1097
Length-at-puberty (cm)	159.1	155.4	151.9	148.8	145.9

however, estimated food availability plunged to $f < 0.75$. The plunge had dramatic effects on the specific growth rate of the reared fish (Fig. 5); the growth rate dropped from 0.5% body mass per day for 450 days old (around 66 cm fork length), to just 0.1% for the 750 days old (around 81 cm fork length) tuna. Our model suggested that for $f > 0.9$ rates greater than 0.3% per day could have been obtained. Such high growth rates have been observed for reared Atlantic bluefin tuna (Tičina et al., 2007). Though comparisons between different species should not be taken at face value, the combination of theoretical results and evidence from Atlantic bluefin tuna strongly suggested that PBT was substantially underfed during the second year.

During the third year of rearing, food availability improved noticeably. The diet remained sardine-dominated, but also included a considerable fraction of bonito and other bait fish (Table 2), and the specific growth rate increased to almost 0.14% body mass per day for the 1050 days old tuna (around 91 cm fork length). However, the rate was still lower than the theoretically possible 0.3% for $f > 0.9$, and the rate of 0.20 and 0.30% body mass per day observed in Atlantic bluefin tuna of age 2 at 18.1 and 19.1 °C (Tičina et al., 2007). Hence, the fish likely remained somewhat underfed with the sardine-dominated diet in year three. From the fourth year onward, food availability showed an improving trend, aside from a small dip in the fifth year and another larger dip in the seventh year of the rearing cycle. The diet in year four consisted of mackerel, horse mackerel, bonito, and other bait fish, and in years five and six of sardine, horse mackerel, and mackerel (Table 2). Afterward, the diet progressively shifted to being mackerel-dominated. Relatively high estimates of food availability towards the end of the rearing cycle confirmed that a mackerel-dominated diet, provided in sufficient quantities, could sustain large PBT individuals held in captivity. We found the dip in year seven particularly interesting because of a possible connection with the overestimate of the maturity-at-puberty parameter (E_H^p) and the way the model handled the initial investment into the reproduction buffer.

A potential overestimate of E_H^p could be partly responsible for the dip in the reconstructed food availability in year seven. The reproduction buffer (E_R) represents an important contribution to the modeled body mass (Eq. (2)). However, the model does not recognize the existence of the buffer as long as the fish are immature ($E_H < E_H^p$). Hence, if the estimated E_H^p is too high, the feeding history reconstruction algorithm compensates for the missing mass contribution by increasing predicted food availability. As the level of maturity finally reaches E_H^p, the reproduction buffer is accounted for, but at a food availability that is slightly too high because of the previous overcompensation. If continued, the higher food availability would produce too much weight in the reproductive buffer, so the algorithm has to compensate in the other direction, lowering the estimate of food availability and potentially contributing to the dip in year seven.

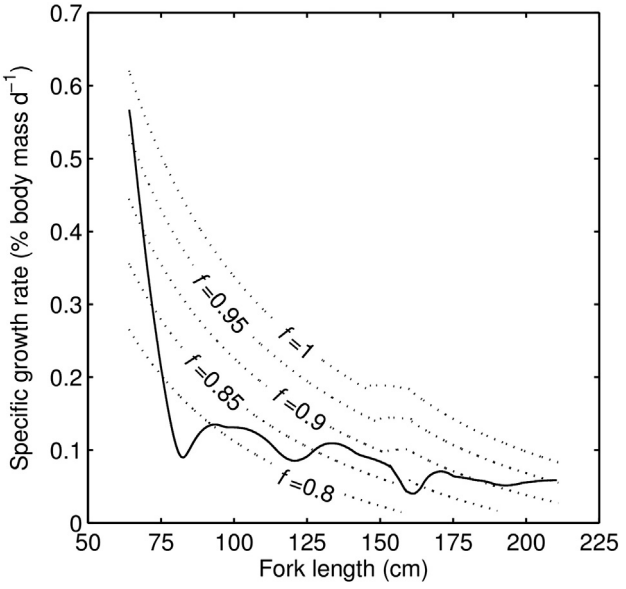

Fig. 5. Specific growth rate at reconstructed (solid line) and several constant (dotted lines) food availabilities. When $f = 0.8$ PBT grows to about 165 cm fork length.

Aforementioned underfeeding during the early development is the likely culprit for the long maturation time (age-at-puberty) of almost seven years, compared to as low as three years in cultured fish (Hirota et al., 1976) and five or (at most) six years in the wild (Chen et al., 2006; Jusup et al., 2011). To elaborate, in Table 4 we present theoretical predictions of age-at-puberty as a function of food availability. At $f = 0.8$, puberty is reached 4705 days after hatching at 159.1 cm fork length, which is very close to the ultimate length at this food level. If f was just slightly lower, there would not be enough energy for PBT to mature. At $f = 0.85$, puberty is reached 2450 days after hatching, and at $f = 0.9$, the modeled age-at-puberty decreases to 1726 days after hatching, indicating just how much suboptimal feeding can affect the development of captive PBT. We suggest that the period of feeding with f close to 0.75 not only stifled growth, but also delayed fish maturation.

Before steering the discussion to energy conversion efficiencies, it is important to address the limitations of our approach. In particular, the model validation can be better understood when considered in conjunction with the potential sources of error:

1. At least three parameters set to a constant value are, in reality, diet-specific: (i) gastric evacuation rates in PBT decrease considerably when prey has an exoskeleton or a high level of lipids (Butler et al, 2010), thus affecting the maximum surface-area-specific assimilation rate, $\{\dot{p}_{Am}\}$; (ii) assimilation efficiency, κ_X, depends on the diet because the chemical composition of feed is much more variable than the chemical composition of PBT tissue (Sterner and George, 2000), implying that varying degrees of conversion are necessary; and (iii) the mass–energy coupler for food, ρ_X, describes energy per unit of mass of feed and, therefore, is directly affected by the feed composition.
2. Though seawater temperature could have affected growth rates (Katavić et al., 2003; Masuma et al., 2008), in simulations we used the average of approximately 21 °C recorded on site. Using the average is justifiable when the time scale of temperature oscillations is shorter than the temporal resolution of the data. In our case, only the annual growth data were available, whereas the daily average temperature at the PBT facility oscillated sinusoidally between 16 and 26 °C over the year (Miyashita, 2002). If, however, prolonged periods of time with unusually low or high seawater temperature had occurred, the model would have predicted anomalous quantities of ingested feed.
3. Estimates of feed depend on the number of individuals in net pens, which may not have been correct at all times. Only one count was available each year, and we interpolated the numbers by assuming constant mortality in-between. If the interpolated values differed considerably from the actual numbers in net pens, estimate of the total ingestion rate and, therefore, model outputs would be affected.
4. We assumed that all distributed feed had been ingested, but large amount of feed could have remained uneaten (Mylonas et al., 2010). Aquaculture facilities usually avoid uneaten feed because it presents an unnecessary cost and raises environmental concerns. Good cultivation practices nowadays result in relatively small amounts of uneaten feed (Vita et al., 2004). Nonetheless, some differences between the amounts of distributed and ingested feed do exist,

Please cite this article as: Jusup, M., et al., Simple measurements reveal the feeding history, the onset of reproduction, and energy conversion efficiencies in captive bluefin tuna, J. Sea Res. (2014), http://dx.doi.org/10.1016/j.seares.2014.09.002

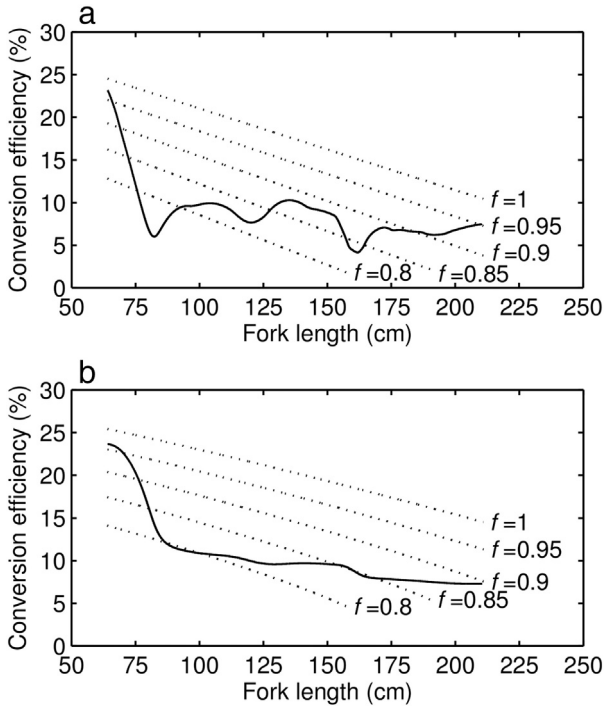

Fig. 6. Energy conversion efficiencies at reconstructed (solid line) and several constant (dotted lines) food availabilities: a) the instantaneous conversion efficiency and b) the cumulative conversion efficiency. When $f = 0.8$ PBT grows to about 165 cm fork length.

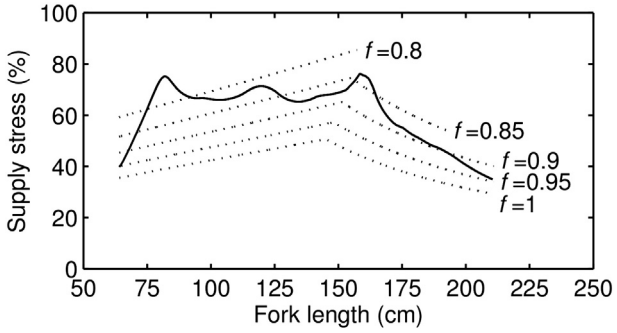

Fig. 7. Supply stress at reconstructed (solid line) and several constant (dotted lines) food availabilities expressed as a percentage of the theoretical maximum of 4/27. When $f = 0.8$ PBT grows to about 165 cm fork length.

and may turn out to be considerable — especially when aiming at high food availability.

We refrained from adjusting the model to explicitly account for any of the above sources of error because doing so could have ultimately undermined the credibility of our approach. Assuming, for instance, that the value of ρ_X changed with the diet of PBT broodstock from year to year would amount to little more than adding extra parameters to the model. Given enough parameters, however, any dataset could be fitted perfectly, thus defeating the purpose of validation which was to demonstrate that the model performed reasonably well under a set of limiting assumptions. Therefore, all parameters were independently estimated, and only the feeding history was fitted from the present data. Extra parameters that could have produced a better fit were not considered because we would need to fit them using the same rather limited data set, which in turn would make our insights speculative at best and even misleading at worst.

3.2. Energy conversion efficiencies and the supply stress

Instantaneous (Fig. 6a) and cumulative (Fig. 6b) energy conversion efficiencies were calculated using Eqs. (6a) and (6b), respectively. For the reconstructed theoretical feeding history, $f_P(t)$, both conversion efficiencies dropped considerably in the first 80 days, and then retained relatively low values throughout the rearing cycle. The instantaneous conversion efficiency was much more responsive to the changes in food availability, largely because of the small energy reserve capacity of PBT (noted by Jusup et al., 2011). By contrast, the cumulative conversion efficiency, reflecting the entire feeding history, could not be tweaked by short term improvements in feeding conditions. As an example, the instantaneous conversion efficiency from around 125 to 155 cm fork length – a period of 690 days – was well above the reference level for the fish constantly fed at $f = 0.85$, yet the cumulative conversion efficiency barely reached this reference level by the end of the same period. These results suggested that a period of suboptimal feeding could not be easily offset, and therefore had long-term negative consequences on the cultivation process.

PBT utilize only a small fraction of energy from the reserve to increase the amount of the structure. Even in relatively small PBT (<75 cm fork length), less than 25% of energy mobilized from the reserve is allocated to growth (Fig. 6). The instantaneous conversion efficiency drops to around 10% in large fish (>200 cm fork length) even at the highest possible food availability. Similarly, the cumulative conversion efficiency in the limit $f \to 1$ shows that, depending on the body length, only somewhere between 25 and 15% of the total energy mobilized from the reserve is available for growth. These results provide the theoretical underpinning for estimates made on yellowfin tuna using a more traditional bioenergetic framework in which around 6% of the total metabolic rate is allocated to growth (Korsmeyer and Dewar, 2001; for a comparison of bioenergetic approaches see Nisbet et al, 2012). A related implication is that feed conversion ratios in tuna aquaculture must be high (Naylor and Burke, 2005).

The supply stress in the case of PBT (Fig. 7) was found to be relatively high and very sensitive to food availability. At the reconstructed $f_P(t)$, the supply stress quickly increased from 40% to almost 80% of the theoretical maximum early into the rearing cycle and then oscillated around 70% throughout the juvenile stage, confirming just how little energy was left for growth and maturation of the studied PBT broodstock. Simulations further indicated that at $f = 0.8$ (i.e. at 80% of the maximum feeding rate at a given temperature) there was barely enough energy for PBT to reach puberty. Even in the limit $f \to 1$, the stress crossed 40% of the maximum near length-at-puberty. In terms of food availability, therefore, PBT metabolism was found to be very restrictive, with continuous high level of food uptake required for favorable growth and maturation.

Conversion efficiencies are expected to decrease with body length because the larger the structure, the more energy is required for somatic maintenance, leaving less for growth. At given body length, conversion efficiencies are also expected to decrease with decreasing food availability. The reason can be understood by considering that somatic maintenance costs (in DEB theory) depend on the structural length, but not on food availability or energy reserves. The utilization flow, on the other hand, *is* dependent on the state of energy reserves and consequently decreases with decreasing food availability. The combination of stable somatic maintenance and the declining utilization flow ultimately results in less energy for growth. In nature, however, the situation may be more complex. Tunas exhibit behavioral adjustments when food level is very low, presumably aimed at conserving energy. Starving skipjack (*Katsuwonus pelamis*), kawakawa (*Euthynnus affnis*), and yellowfin (*T. albacares*) tunas are known to decrease their swimming speed almost to the minimum needed for maintaining neutral buoyancy (Boggs and Kitchell, 1991). Hence, somatic maintenance costs independent of variables other than the structural length may be just a reasonable first approximation. If under certain environmental conditions, e.g. restricted food supply, this approximation faltered, we would be left with biased estimates of energy conversion efficiencies.

Please cite this article as: Jusup, M., et al., Simple measurements reveal the feeding history, the onset of reproduction, and energy conversion efficiencies in captive bluefin tuna, J. Sea Res. (2014), http://dx.doi.org/10.1016/j.seares.2014.09.002

More importantly, we would have a confirmation that our understanding of the components of somatic maintenance is due for an update (see also Nisbet et al, 2012).

The analysis of energy conversion and the supply stress in PBT suggests that maximizing the efficiency of the rearing cycle requires maintaining food availability as high as practically possible. Aiming for the limit $f \to 1$, however, may not be a feasible strategy because getting the fish to eat the necessary amount of feed would likely increase the amount of uneaten feed and/or demand more than one feeding session a day. The consequent negative effect on operational costs and environmental impacts may surpass savings attained through the improved efficiency. Furthermore, reduced feeding of reared fish may result in considerable health benefits for the fish as outlined in a preliminary study performed on juvenile Atlantic bluefin tuna in the Adriatic Sea (Mišlov Jelavić et al., 2012). Because in DEB theory reduced feeding implies lower metabolic rates, which in turn are linked with prolonged life expectancy (van Leeuwen et al., 2010), the relationship between feeding rates and health benefits may represent an exciting direction not only for experimental, but also for DEB-based theoretical studies.

4. Conclusion

We have used length and weight of the fish, i.e. data commonly available at aquaculture facilities, in conjunction with a previously set up bioenergetic model for Pacific bluefin tuna to reconstruct the feeding history of a captive PBT broodstock. The reconstructed theoretical feeding history was then compared with the actual quantities. A goodness-of-fit analysis confirmed the satisfactory predictive power and, in turn, provided an independent validation of the model performance. Based on these results we concluded that simple measurements revealed the feeding history of captive PBT. The same procedure could be applied to other reared fish species.

Given that DEB-based models account for the investment of energy into maturation and reproduction, we were able to use the reconstructed theoretical feeding history to predict the age-at-puberty of the studied PBT broodstock. The predicted age was surprisingly high considering known PBT maturation times, but agreed well with the time to the first observed reproductive event. This surprising, but accurate, result additionally confirmed the model validity and suggested that simple measurements could be used to predict the onset of reproduction in captive PBT.

By relating growth and utilization energy flows, we estimated the fraction of energy from the reserve invested into growth of the studied PBT broodstock. These quantities, interpreted as energy conversion efficiencies, showed two interesting properties. First, upper limits of conversion efficiencies were remarkably low, in line with findings from respirometry-based studies on smaller yellowfin tuna (Korsmeyer and Dewar, 2001) and high feed conversion ratios recorded in tuna aquaculture (Naylor and Burke, 2005). Second – an apparently undocumented phenomenon – efficiencies in the juvenile fish fell rapidly with food availability, resulting in the modest specific growth rate even though the feeding rate was at all times above approximately 75% of the maximum (Fig. 2). These findings confirm that bluefin tuna aquaculture is a resource-intensive process that requires precise definition of good rearing practices to avoid unnecessary costs associated with suboptimal efficiency.

In the context of good rearing practices, the modeled conversion efficiencies are the highest in the limit $f \to 1$, yet concluding that aquaculture production should aim for this limit may represent a naive interpretation of the results. Among several reasons for thinking so, the most intriguing are the potential health benefits for the fish observed during reduced feeding (Mišlov Jelavić et al., 2012). For DEB-based models to capture such subtle effects and escape the danger of naive interpretations, a convincing link between organismal energetics and a health indicator (e.g. the concentration of damage inducing compounds) would have to be established. We believe this to be a promising line of future research, especially because the results may prove useful far beyond the confines of aquaculture production (see Nisbet et al., 2000).

Acknowledgments

We thank SALM Kooijman for constructive criticism. This work was supported in part by the Global Center of Excellence (GCOE) Program No. K07 "Asian Conservation Ecology". Japan Society for the Promotion of Science (JSPS) Postdoctoral Fellowship Program for Foreign Researchers (P13380) and the accompanying Grant-in-Aid for Scientific Research allowed M.J. to conduct research in Japan.

Appendix A

The DEB model for PBT was inspired by the standard DEB representation (Kooijman, 2010) and, therefore, bears considerable similarities with all DEB-based models. In particular, we assume that the fish can be conceptually divided into two compartments distinguished by their dynamics: the reserve and the structure. Energy from the assimilated food is first deposited in the reserve compartment and then mobilized to fuel metabolic processes, including the growth of the structure. The reserve does not require any energy expenditure on its maintenance. By contrast, the structure requires continuous maintenance and grows by receiving energy mobilized from the reserve as a function of both the current size of the structure and the current state of the reserve. We further assume that maturation is caused by the corresponding investment of energy mobilized from the reserve. The state of an individual fish, therefore, is fully determined by three variables: the amount of energy in the reserve (E), the structural volumetric length (L), and the level of maturity (E_H). Upon the onset of reproduction, energy that was previously invested in maturation is assumed to be stored in the reproduction buffer until getting released in the form of eggs during the next reproductive season. To track the state of the reproduction buffer, an auxiliary variable (E_R) needs to be introduced. The model state variables, together with the corresponding units, are conveniently summarized in Table A1.

The dynamics of the state variables is controlled by six energy flows (Fig. 1). For the reserve compartment, we have

$$\frac{dE}{dt} = \dot{p}_A - \dot{p}_C, \tag{A1}$$

where $\dot{p}_A$ and $\dot{p}_C$ are assimilation and utilization energy flows, respectively. An equivalent equation for the dynamics of the reserve density, $[E] = E / L^3$, is

$$\frac{d[E]}{dt} = \frac{\dot{p}_A - \dot{p}_C}{L^3} - 3[E]\frac{d}{dt}\ln L. \tag{A2}$$

The differential equation for the structure compartment can be written in the form

$$\frac{dL}{dt} = \frac{\dot{p}_G}{3L^2[E_G]}, \tag{A3}$$

where $\dot{p}_G$ is the growth energy flow and $[E_G]$ is the volume-specific cost of structure. Finally, the equation for maturity is

$$\frac{dE_H}{dt} = \dot{p}_R \tag{A4}$$

when $E_H < E_H^p$, where $\dot{p}_R$ is the maturation energy flow and E_H^p is the maturity-at-puberty. The κ-rule connects growth and maturation flows with the utilization flow:

$$\dot{p}_G = \kappa\dot{p}_C - \dot{p}_S, \tag{A5a}$$

$$\dot{p}_R = (1-\kappa)\dot{p}_C - \dot{p}_J, \tag{A5b}$$

Please cite this article as: Jusup, M., et al., Simple measurements reveal the feeding history, the onset of reproduction, and energy conversion efficiencies in captive bluefin tuna, J. Sea Res. (2014), http://dx.doi.org/10.1016/j.seares.2014.09.002

Table A1
List of symbols, formulas, and values (at the reference temperature of 20 °C).

Description	Unit	Symbol, formula, value
Amount of energy in the reserve	J	E, Eq. (A1)
Energy density	$J \cdot cm^{-3}$	$[E] = E / L^3$, also see Eq. (A2)
Structural volumetric length	cm	L, Eq. (A3)
Level of maturity	J	E_H, Eq. (A4)
Status of the reproduction buffer	J	$E_R = \int \dot{p}_R dt$ when $E_H \geq E_H^p$
Assimilation flow	$J \cdot d^{-1}$	$\dot{p}_A = \{\dot{p}_{Am}\} f L^2$
Utilization (mobilization) flow	$J \cdot d^{-1}$	$\dot{p}_C = E(\dot{v}[E_G]L^2 + \dot{p}_S) / (\kappa E + [E_G]L^3)$
Somatic maintenance flow	$J \cdot d^{-1}$	$\dot{p}_S = \dot{p}_M + \dot{p}_T = [\dot{p}_M]L^3 + \{\dot{p}_T\}L^2$
Maturity maintenance flow	$J \cdot d^{-1}$	$\dot{p}_J = k_J E_H$
Growth flow	$J \cdot d^{-1}$	$\dot{p}_G$, Eq. (A5a)
Maturation (reproduction) flow	$J \cdot d^{-1}$	$\dot{p}_R$, Eq. (A5b)
Shape correction function	–	$M_1(L, E_H)$, Eq. (A8)
Shape factor	–	$\delta_M(E_H)$, Eq. (A9)
Thermogenic efficiency	–	$M_2(E_H)$, Eq. (A10)
Max. surf.-area-specific assimilation rate[a]	$J \cdot cm^{-2} \cdot d^{-1}$	$\{\dot{p}_{Am}\}$, 160.53
Volume-specific cost of structure	$J \cdot cm^{-3}$	$[E_G]$, 8828
Energy conductance[a]	$cm \cdot d^{-1}$	$\dot{v}$, 0.2386
Volume-specific somatic maintenance rate[a]	$J \cdot cm^{-3} \cdot d^{-1}$	$[\dot{p}_M]$, 12.842
Surf.-area-specific somatic maintenance rate[a]	$J \cdot cm^{-2} \cdot d^{-1}$	$\{\dot{p}_T\}$,1635.6
Maturity maintenance rate coefficient[a]	d^{-1}	k_J, 0.045166
Reserve allocation to soma	–	κ, 0.7807
Maturity-at-birth/-puberty	J	E_H^b, 0.7637 / E_H^p, $2.548 \cdot 10^7$
Other maturities	J	E_H^l, $6.902 \cdot 10^3$ / $E_H{}^2$, $5.402 \cdot 10^5$ / E_H^v, $9.695 \cdot 10^5$
Density of the structure	$g \cdot cm^{-3}$	d_V, 1
Mass-energy coupler for the reserve/food	$g \cdot J^{-1}$	ρ_E, $1.0864 \cdot 10^{-4}$ / ρ_X, $1.894 \cdot 10^{-4}$
Assimilation efficiency	–	$\kappa_X = 0.8$
Shape factor in the larval/adult stage	–	$\delta_M{}^1 = 0.2249$ / $\delta_M{}^2 = 0.2704$

The conversion factor, C_T, from the reference temperature, T_{ref}, to another temperature, T, is given by the Arrhenius relationship $C_T = \exp(T_A / T_{ref} - T_A / T)$. The Arrhenius temperature for PBT is $T_A \approx 5300$ K.

[a] Three rate parameters, energy conductance, and maturity maintenance rate coefficient are temperature-dependent.

where $\dot{p}_S$ and $\dot{p}_J$ are somatic and maturity maintenance energy flows, respectively, and $0 < \kappa < 1$ is a constant. To make Eqs. (A1–A5b) solvable using numerical methods, we need to specify how $\dot{p}_A$, $\dot{p}_C$, $\dot{p}_S$, and $\dot{p}_J$ depend on the state variables.

The assimilation flow ($\dot{p}_A$) is the amount of energy stored in the reserve per unit of time. Though energy is originally acquired through feeding, the assimilation flow differs from the amount of ingested energy per unit of time (i.e. the ingestion rate) at least partly because of an inefficient digestive system and the chemical transformation of food into the reserve. The difference between ingested and assimilated energy is called the assimilation overhead. To get a mathematical expression for the assimilation flow we make two assumptions. First, because ingestion takes place at the surface separating the fish from the environment, the ingestion rate is assumed to be proportional to the squared structural length. The proportionality constant is commonly separated into two factors; the maximum surface-area-specific ingestion rate, $\{\dot{p}_{Xm}\}$, represents the physiological limitations of the digestive system, whereas food availability, $0 \leq f \leq 1$, reflects the environmental conditions. The second assumption is that the constant fraction of the ingestion rate is used to cover the assimilation overhead. Consequently, we can introduce the assimilation efficiency of food into the reserve, $0 < \kappa_X \leq 1$, so that the maximum surface-area-specific assimilation rate is given by $\{\dot{p}_{Am}\} = \kappa_X\{\dot{p}_{Xm}\}$. The resulting expression for the assimilation flow is shown in Table A1.

Energy from the reserve is used to power various metabolic processes at a rate determined by the utilization (or mobilization) energy flow ($\dot{p}_C$). We can find a mathematical expression for the utilization flow by assuming that the reserve density follows a first order dynamics (van der Meer, 2006). In other words, when there is no food in the environment, the reserve density decreases at a rate proportional to the current amount of the reserve density. Eq. (A2) then implies

$$\frac{\dot{p}_C}{L^3} + 3[E]\frac{d}{dt}\ln L = C[E], \tag{A6}$$

where $C = C(L)$ is temporarily an unknown function of L. To solve for C, we plug Eq. (A6) into Eq. (A2) and observe that the reserve density is in the equilibrium at a level $[E]^*$ given by $C[E]^* = \dot{p}_A / L^3$. When the food availability is at maximum, i.e. $f = 1$, the equilibrium reserve density should also reach its maximum, i.e. $[E]^* = [E_m]$. Consequently, $C = \{\dot{p}_{Am}\} / [E_m]L$ which upon inserting into Eq. (A6) gives

$$\dot{p}_C = E\left(\frac{\{\dot{p}_{Am}\}}{[E_m]L} - 3\frac{d}{dt}\ln L\right). \tag{A7}$$

The ratio of the maximum surface-area-specific assimilation rate and the maximum reserve density, commonly denoted by $\dot{v}$, is called the energy conductance. Using Eqs. (A3) and (A5a), it is possible to transform Eq. (A7) into the form given in Table A1.

Next, we turn our attention to energy flows that cover the maintenance costs, i.e. keep the fish alive and healthy. As indicated before, we recognize the two types of maintenance energy flows. The bulk of the somatic maintenance flow ($\dot{p}_S$) is assumed to originate from continuous degradation and synthesis of proteins collectively known as the protein turnover. The energetic costs of the protein turnover rise in proportion to the number of cells, which in turn is approximately proportional to the cubed structural length. In addition, all tuna species are capable of thermogenesis, implying that enough energy is dissipated to counteract the heat loss through the outer surface. Such an energy expenditure needs to be proportional only to the squared structural length. We thus make a distinction between the volume-related ($\dot{p}_M$) and surface-area-related ($\dot{p}_T$) somatic maintenance costs, where $\dot{p}_S = \dot{p}_M + \dot{p}_T$ with $\dot{p}_M \propto L^3$ and $\dot{p}_T \propto L^2$. Proportionality constants $[\dot{p}_M]$ and $\{\dot{p}_T\}$ are called the volume-specific and the surface-area-specific somatic maintenance costs, respectively. As for the maturity maintenance flow ($\dot{p}_J$), we first note that the level of maturity is identified with the complexity of the structure, which – in line with the second law of thermodynamics – would decrease without some form of maintenance (Sousa et al., 2008, 2010). We assume that the maturity maintenance flow is proportional to the current level of maturity, i.e. $\dot{p}_J \propto E_H$, where the

Please cite this article as: Jusup, M., et al., Simple measurements reveal the feeding history, the onset of reproduction, and energy conversion efficiencies in captive bluefin tuna, J. Sea Res. (2014), http://dx.doi.org/10.1016/j.seares.2014.09.002

proportionality constant $\dot{k}_J$ is the maturity maintenance rate coefficient. Mathematical expressions originating from the above considerations are conveniently summarized in Table A1.

Eqs. (A1)–(A5b) and energy flows in Table A1 provide us with all ingredients necessary to run the standard DEB model, but are insufficient to account for the specifics of PBT physiology. These specifics come into play when trying to model the whole life cycle of a fish because some parameter values that are valid during early development become invalid for a more mature individual. For example, due to tremendous physiological and anatomical changes, we model larval PBT as a V1-morphic organism, which means that the maximum surface-area-specific assimilation rate and the energy conductance in all equations need to be multiplied by an auxiliary function

$$M_1(L,E_H)=\begin{cases}1, & E_H<E_H^b\\ L/L_b, & E_H^b\le E_H<E_H^j\\ L_j/L_b, & E_H^j\le E_H\end{cases}, \tag{A8}$$

where L_b (L_j) is the structural length at which the level of maturity reaches the maturity-at-birth, E_H^b (maturity-at-metamorphosis, E_H^j). The auxiliary function $M_1 = M_1(L, E_H)$ is called the shape correction function. Another parameter that changes with maturity in the case of PBT is the shape factor (δ_M). This parameter connects the structural length to a well-defined, measurable length (L_w) through the relationship $\delta_M = L / L_w$. For an isomorph, the ratio of any two length measures, including the shape factor, is constant throughout the lifetime. Larval PBT, however, undergo anatomical changes that result in the allometric growth of various body parts. Even for young juveniles isomorphism is only the first approximation. As a consequence, we introduce the relationship

$$\delta_M(E_H)=\frac{\delta_M^1\left(E_H^2-E_H^b\right)+\delta_M^2\left(E_H-E_H^b\right)}{E_H+E_H^2-2E_H^b},\ E_H^b\le E_H<E_H^p, \tag{A9}$$

where $\delta_M{}^1$ ($\delta_M{}^2$) is the larval (adult) shape factor and $\delta_M(E_H{}^2) = (\delta_M{}^1 + \delta_M{}^2) / 2$. One last parameter that requires a correction as the fish matures is the surface-area-specific somatic maintenance rate. Thermogenesis, though not present in larval PBT, becomes readily observable in young juvenile fish, approximately 80 to 120 days after hatching. To account for the effects of thermogenic energy dissipation on the energy budget, we introduce another auxiliary function

$$M_2(E_H)=\begin{cases}0, & E_H<E_H^j\\ \left(E_H-E_H^j\right)/\left(E_H^y-E_H^j\right), & E_H^j\le E_H<E_H^y\\ 1, & E_H^y\le E_H\end{cases}, \tag{A10}$$

where E_H^y is the maturity at which thermogenesis is fully developed. The auxiliary function $M_2 = M_2(E_H)$ can be interpreted as the thermogenic efficiency.

References

Aguado, F., Martínez, F.J., García-García, B., 2004. In vivo total nitrogen and total phosphorus digestibility in Atlantic bluefin tuna (*Thunnus thynnus thynnus* Linnaeus, 1758) under industrially intensive fattening conditions in Southeast Spain Mediterranean coastal waters. Aquat. Nutr. 10 (6), 413–419.

Aguado-Giménez, F., García-García, B., 2003. Macronutrient composition of food for bluefin tuna (*Thunnus thynnus thynnus*) fattening. Cah. Options Méditerr. 60, 15–16.

Augustine, S., Gagnaire, B., Floriani, M., Adam-Guillermin, C., Kooijman, S.A.L.M., 2011. Developmental energetics of zebrafish, *Danio rerio*. Comp. Biochem. Physiol. A Mol. Integr. Physiol. 159 (3), 275–283.

Augustine, S., Gagnaire, B., Adam-Guillermin, C., Kooijman, S.A.L.M., 2012. Effects of uranium on the metabolism of zebrafish, *Danio rerio*. Aquat. Toxicol. 118, 9–26.

Bavčević, L., Klanjšček, T., Karamarko, V., Aničić, I., Legović, T., 2010. Compensatory growth in gilthead seabream (*Sparus aurata*) compensates weight, but not length. Aquaculture 301 (1–4), 57–63.

Boggs, C.H., Kitchell, J.F., 1991. Tuna metabolic rates estimated from energy losses during starvation. Physiol. Zool. 64 (2), 502–524.

Boggs, P.T., Tolle, J.W., 1995. Sequential quadratic programming. Acta Numer. 4 (1), 1–51.

Butler, C.M., Rudershausen, P.J., Buckel, J.A., 2010. Feeding ecology of Atlantic bluefin tuna (*Thunnus thynnus*) in North Carolina: diet, daily ration, and consumption of Atlantic menhaden (*Brevoortia tyrannus*). Fish. Bull. 108 (1), 56–69.

Carter, C.G., Bransden, M.P., Van Barneveld, R.J., Clarke, S.M., 1999. Alternative methods for nutrition research on the southern bluefin tuna *Thunnus maccoyii*: in vitro digestibility. Aquaculture 179 (1), 57–70.

Chen, K.-S., Crone, P., Hsu, C.-C., 2006. Reproductive biology of female Pacific bluefin tuna *Thunnus orientalis* from south-western North Pacific Ocean. Fish. Sci. 72, 985–994.

Clark, T.D., Brandt, W.T., Nogueira, J., Rodriguez, L.E., Price, M., Farwell, C.J., Block, B.A., 2010. Postprandial metabolism of Pacific bluefin tuna (*Thunnus orientalis*). J. Exp. Biol. 213 (14), 2379–2385.

Collette, B.B., Carpenter, K.E., Polidoro, B.A., Juan-Jordá, M.J., Boustany, A., Die, D.J., Elfes, C., Fox, W., Graves, J., Harrison, L.R., et al., 2011. Conservation. High value and long life — double jeopardy for tunas and billfishes. Science 333, 291–292.

De Metrio, G., Bridges, C.R., Mylonas, C.C., Caggiano, M., Deflorio, M., Santamaria, N., Zupa, R., Pousis, C., Vassallo-Agius, R., Gordin, H., Corriero, A., 2010. Spawning induction and large-scale collection of fertilized eggs in captive Atlantic bluefin tuna (*Thunnus thynnus* L.) and the first larval rearing efforts. J. Appl. Ichthyol. 26 (4), 596–599.

Dewar, H., Graham, J.B., 1994. Studies of tropical tuna swimming performance in a large water tunnel. J. Exp. Biol. 192 (1), 13–31.

Einarsson, B., Birnir, B., Sigurðsson, S., 2011. A dynamic energy budget (DEB) model for the energy usage and reproduction of the Icelandic capelin (*Mallotus villosus*). J. Theor. Biol. 281 (1), 1–8.

Fablet, R., Pecquerie, L., de Pontual, H., Høie, H., Millner, R., Mosegaard, H., Kooijman, S.A.L.M., 2011. Shedding light on fish otolith biomineralization using a bioenergetic approach. PLoS ONE 6 (11), e27055.

Fitzgibbon, Q.P., Seymour, R.S., Ellis, D., Buchanan, J., 2007. The energetic consequence of specific dynamic action in southern bluefin tuna *Thunnus maccoyii*. J. Exp. Biol. 210 (2), 290–298.

Freitas, V., Kooijman, S.A.L.M., van der Veer, H.W., 2012. Latitudinal trends in habitat quality of shallow-water flatfish nurseries. Mar. Ecol. Prog. Ser. 471, 203–214.

Fritsch, F.N., Carlson, R.E., 1980. Monotone piecewise cubic interpolation. SIAM J. Numer. Anal. 17 (2), 238–246.

Graham, J.B., Dickson, K.A., 2001. Anatomical and physiological specializations for endothermy. Fish Physiol. Ser. 19, 121–166.

Graham, J.B., Dickson, K.A., 2004. Tuna comparative physiology. J. Exp. Biol. 207, 4015–4024.

Grubišić, L., Šegvić-Bubić, T., Pleić, I.L., Mišlov-Jelavić, K., Tičina, V., Katavić, I., Mladineo, I., 2013. Morphological and genetic identification of spontaneously spawned larvae of captive bluefin tuna in the Adriatic Sea. Fisheries 38 (9), 410–417.

Hirota, H., Morita, M., Taniguchi, N., 1976. An instance of the maturation of 3 full years old bluefin tuna cultured in the floating net. Bull. Jpn. Soc. Sci. Fish. 42, 939.

Iioka, C., Kani, K., Nhhala, H., 2000. Present status and prospects of technical development of tuna sea-farming. Cah. Options Méditerr. 47, 275–285.

Ji, S.C., Takaoka, O., Biswas, A.K., Seoka, M., Ozaki, K., Kohbara, J., Ukawa, M., Shimeno, S., Hosokawa, H., Takii, K., 2008. Dietary utility of enzyme-treated fish meal for juvenile Pacific bluefin tuna *Thunnus orientalis*. Fish. Sci. 74 (1), 54–61.

Juan-Jordá, M.J., Mosqueira, I., Cooper, A.B., Freire, J., Dulvy, N.K., 2011. Global population trajectories of tunas and their relatives. Proc. Natl. Acad. Sci. U. S. A. 108, 20650–20655.

Jusup, M., Klanjšček, J., Petricioli, D., Legović, T., 2009. Predicting aquaculture-derived benthic organic enrichment: model validation. Ecol. Model. 220 (19), 2407–2414.

Jusup, M., Klanjšček, T., Matsuda, H., Kooijman, S.A.L.M., 2011. A full lifecycle bioenergetic model for bluefin tuna. PLoS ONE 6 (7), e21903.

Kaji, T., 2003. Bluefin tuna larval rearing and development — state of the art. Cah. Options Méditerr. 60, 85–89.

Katavić, I., Tičina, V., Franičević, V., 2003. Bluefin tuna (*Thunnus thynnus* L.) farming on the Croatian coast of the Adriatic Sea — present stage and future plans. Cah. Options Méditerr. 60, 101–106.

Katz, S.L., 2002. Design of heterothermic muscle in fish. J. Exp. Biol 205 (15), 2251–2266.

Kooijman, S.A.L.M., 2010. Dynamic Energy Budget Theory for Metabolic Organisation, 3rd edition. Cambridge University Press, Cambridge (532 pp.).

Kooijman, S.A.L.M., Lika, K., 2014. Comparative energetics of the 5 fish classes on the basis of dynamic energy budgets. Journal of Sea Research http://dx.doi.org/10.1016/j.seares.2014.01.015 (in press, ISSN 1385-1101).

Kooijman, S.A.L.M., Pecquerie, L., Augustine, S., Jusup, M., 2011. Scenarios for acceleration in fish development and the role of metamorphosis. J. Sea Res. 66 (4), 419–423.

Korsmeyer, K.E., Dewar, H., 2001. Tuna metabolism and energetics. Fish Physiol. 19, 35–78.

Korsmeyer, K.E., Dewar, H., Lai, N.C., Graham, J.B., 1996. The aerobic capacity of tunas: adaptation for multiple metabolic demands. Comp. Biochem. Physiol. A 113 (1), 17–24.

Kubo, T., Sakamoto, W., Murata, O., Kumai, H., 2008. Whole-body heat transfer coefficient and body temperature change of juvenile Pacific bluefin tuna *Thunnus orientalis* according to growth. Fish. Sci. 74, 995–1004.

Lika, K., Augustine, S., Pecquerie, L., Kooijman, S.A.L.M., 2014. The bijection from data to parameter space with the standard DEB model quantifies the supply–demand spectrum. J. Theor. Biol. 354, 35–47.

Lika, K., Kooijman, S.A.L.M., Papandroulakis, N., 2014. Metabolic acceleration in Mediterranean Perciformes. Journal of Sea Research http://dx.doi.org/10.1016/j.seares.2013.12.012 (ISSN 1385-1101).

Magnuson, J.J., 1973. Comparative study of adaptations for continuous swimming and hydrostatic equilibrium of scombroid and xiphoid fishes. Fish. Bull. 71 (2), 337–356.

Masuma, S., Miyashita, S., Yamamoto, H., Kumai, H., 2008. Status of bluefin tuna farming, broodstock management, breeding and fingerling production in Japan. Rev. Fish. Sci. 16 (1–3), 385–390.

Please cite this article as: Jusup, M., et al., Simple measurements reveal the feeding history, the onset of reproduction, and energy conversion efficiencies in captive bluefin tuna, J. Sea Res. (2014), http://dx.doi.org/10.1016/j.seares.2014.09.002

Masuma, S., Takebe, T., Sakakura, Y., 2011. A review of the broodstock management and larviculture of the Pacific northern bluefin tuna in Japan. Aquaculture 315 (1), 2–8.
Mišlov Jelavić, K., Stepanowska, K., Grubišić, L., Bubić, T.Š., Katavić, I., 2012. Reduced feeding effects to the blood and muscle chemistry of farmed juvenile bluefin tuna in the Adriatic Sea. Aquac. Res. 43 (2), 317–320.
Miyake, P.M., la Serna JM, De, Di Natale, A., Farrugia, A., Katavić, I., Miyabe, N., Ticina, V., 2003. General review of bluefin tuna farming in the Mediterranean area. Collective Volume of Scientific Papers ICCAT 55(1), pp. 114–124.
Miyashita, S., 2002. Studies on the seedling production of the Pacific bluefin tuna, *Thunnus thynnus orientalis*. Bull. Fish. Lab. Kinki Univ. 8 (171 pp. in Japanese).
Miyashita, S., Sawada, Y., Okada, T., Murata, O., Kumai, H., 2001. Morphological development and growth of laboratory-reared larval and juvenile *Thunnus thynnus* (Pisces: Scombridae). Fish. Bull. 99, 601–616.
Mourente, G., Tocher, D.R., 2009. Tuna nutrition and feeds: current status and future perspectives. Rev. Fish. Sci. 17 (3), 373–390.
Mylonas, C.C., De La Gándara, F., Corriero, A., Ríos, A.B., 2010. Atlantic bluefin tuna (*Thunnus thynnus*) farming and fattening in the Mediterranean Sea. Rev. Fish. Sci. 18 (3), 266–280.
Nash, R.D.M., Valencia, A.H., Geffen, A.J., 2006. The origin of Fulton's condition factor — setting the record straight. Fisheries 31 (5), 236–238.
Naylor, R., Burke, M., 2005. Aquaculture and ocean resources: raising tigers of the sea. Annu. Rev. Environ. Resour. 30, 185–218.
Nisbet, R.M., Muller, E.B., Lika, K., Kooijman, S.A.L.M., 2000. From molecules to ecosystems through dynamic energy budget models. J. Anim. Ecol. 69 (6), 913–926.
Nisbet, R.M., Jusup, M., Klanjšček, T., Pecquerie, L., 2012. Integrating dynamic energy budget (DEB) theory with traditional bioenergetic models. J. Exp. Biol. 215, 892–902.
Pecquerie, L., Petitgas, P., Kooijman, S.A.L.M., 2009. Modeling fish growth and reproduction in the context of the Dynamic Energy Budget theory to predict environmental impact on anchovy spawning duration. J. Sea Res. 62 (2), 93–105.
Pecquerie, L., Johnson, L.R., Kooijman, S.A.L.M., Nisbet, R.M., 2011. Analyzing variations in life-history traits of Pacific salmon in the context of Dynamic Energy Budget (DEB) theory. J. Sea Res. 66 (4), 424–433.
Portilla, E., Tett, P., 2007. Assessing goodness of fit for ECASA models (ECASA internal paper). School of Life Sciences. Napier University, Edinburgh (EH10 5DT).
Roberts, J.L., 1975. Active branchial and ram gill ventilation in fishes. Biol. Bull. 148 (1), 85–105.
Rooker, J.R., Alvarado Bremer, J.R., Block, B.A., Dewar, H., De Metrio, G., Corriero, A., Kraus, R.T., Prince, E.D., Rodriguez-Marin, E., Secor, D.H., 2007. Life history and stock structure of Atlantic bluefin tuna (*Thunnus thynnus*). Rev. Fish. Sci. 15 (4), 265–310.
Sawada, Y., Okada, T., Miyashita, S., Murata, O., Kumai, H., 2005. Completion of the Pacific bluefin tuna *Thunnus orientalis* (Temminck et Schlegel) life cycle. Aquac. Res. 36, 413–421.
Serpa, D., Pousão Ferreira, P., Ferreira, H., da Fonseca, L.C., Dinis, M.T., Duarte, P., 2012. Modelling the growth of white seabream (*Diplodus sargus*) and gilthead seabream (*Sparus aurata*) in semi-intensive earth production ponds using the Dynamic Energy Budget approach. J. Sea Res. 76, 135–145.
Shimose, T., Tanabe, T., Chen, K.-S., Hsu, C.-C., 2009. Age determination and growth of Pacific bluefin tuna, *Thunnus orientalis*, off Japan and Taiwan. Fish. Res. 100, 134–139.
Smith, N.P., Barclay, C.J., Loiselle, D.S., 2005. The efficiency of muscle contraction. Prog. Biophys. Mol. Biol. 88 (1), 1–58.
Sousa, T., Domingos, T., Kooijman, S.A.L.M., 2008. From empirical patterns to theory: a formal metabolic theory of life. Philos. Trans. R. Soc.B Biol. Sci. 363 (1502), 2453–2464.
Sousa, T., Domingos, T., Poggiale, J.-C., Kooijman, S.A.L.M., 2010. Dynamic energy budget theory restores coherence in biology. Philos. Trans. R. Soc.B Biol. Sci. 365 (1557), 3413–3428.
Sterner, R.W., George, N.B., 2000. Carbon, nitrogen, and phosphorus stoichiometry of cyprinid fishes. Ecology 81, 127–140.
Teal, L.R., Hal, R., Kooten, T., Ruardij, P., Rijnsdorp, A.D., 2012. Bio-energetics underpins the spatial response of North Sea plaice (*Pleuronectes platessa* L.) and sole (*Solea solea* L.) to climate change. Glob. Chang. Biol. 18 (11), 3291–3305.
Tičina, V., Katavić, I., Grubišić, L., 2007. Growth indices of small northern bluefin tuna (*Thunnus thynnus*, L.) in growth-out rearing cages. Aquaculture 269 (1), 538–543.
van der Meer, J., 2006. An introduction to Dynamic Energy Budget (DEB) models with special emphasis on parameter estimation. J. Sea Res. 56, 85–102.
van der Meer, J., van der Veer, H.W., Witte, J.I., 2011. The disappearance of the European eel from the western Wadden Sea. J. Sea Res. 66 (4), 434–439.
van der Veer, H.W., Cardoso, J.F., Peck, M.A., Kooijman, S.A.L.M., 2009. Physiological performance of plaice *Pleuronectes platessa* (L.): a comparison of static and dynamic energy budgets. J. Sea Res. 62 (2), 83–92.
van Leeuwen, I.M., Vera, J., Wolkenhauer, O., 2010. Dynamic energy budget approaches for modelling organismal ageing. Philos. Trans. R. Soc.B Biol. Sci. 365 (1557), 3443–3454.
Vita, R., Marin, A., Jiménez-Brinquis, B., Cesar, A., Marín-Guirao, L., Borredat, M., 2004. Aquaculture of Bluefin tuna in the Mediterranean: evaluation of organic particulate wastes. Aquac. Res. 35 (14), 1384–1387.

Please cite this article as: Jusup, M., et al., Simple measurements reveal the feeding history, the onset of reproduction, and energy conversion efficiencies in captive bluefin tuna, J. Sea Res. (2014), http://dx.doi.org/10.1016/j.seares.2014.09.002